

# Hyperfine measurement of $6P_{1/2}$ state in $^{87}\text{Rb}$ using double resonance on blue and IR transition

Elijah Ogaro Nyakang'o,<sup>1</sup> Dangka Shylla,<sup>1</sup> Vasant Natarajan,<sup>2</sup> and Kanhaiya Pandey<sup>1,\*</sup>

<sup>1</sup>*Department of Physics, Indian Institute of Technology Guwahati, Guwahati, Assam 781039, India*

<sup>2</sup>*Department of Physics, Indian Institute of Science, Bangalore, 560012, India*

(Dated: January 19, 2021)

In this paper, we present the spectroscopy of  $6P_{1/2}$  state in  $^{87}\text{Rb}$  using double resonance technique at 780 nm and 421 nm. The double resonance technique is implemented using electromagnetically induced transparency (EIT) and optical pumping methods. Using these spectroscopy methods, we have measured the hyperfine splitting of  $6P_{1/2}$  state with precision of  $<400$  kHz which agrees well with other spectroscopy methods such as electrical discharge and saturated absorption spectroscopy at 421 nm.

PACS numbers:

## I. INTRODUCTION

Precise measurements of the hyperfine structure of various lines in an atom provide key information about the properties of the nucleus such as the electric and magnetic moments. Rb is one of the most widely investigated elements in atomic physics for the spectroscopy both experimentally [1–6] and theoretically [7]. This provides great opportunities to verify different methods of theoretical many-body calculations [8, 9]. Hyperfine splitting measurements are good sources of input for studying subjects at the interface of atomic and nuclear physics such as atomic parity violation [10]. Experimentally, hyperfine structures of  $5P_{3/2}$ ,  $5D_{3/2}$  and  $7S_{1/2}$  have been measured using single-photon transition  $5S_{1/2} \rightarrow 5P_{3/2}$  at 780 nm [1–3], and two-photon transitions  $5S_{1/2} \rightarrow 5D_{3/2}$  at 778 nm [4] and  $5S_{1/2} \rightarrow 7S_{1/2}$  at 760 nm [2, 5, 6] respectively.

Besides verifying theoretical calculations, the above referred transitions are used as low cost optical frequency standards. For example, the precisely measured transition  $5S_{1/2} \rightarrow 5P_{3/2}$  at 780 nm is used as an optical reference for measuring unknown transitions [3]. All these transitions fall in IR region; however, the weak and narrow linewidth ( $2\pi \times 1.27$  MHz [11]) transition in the blue region (i.e. at 421 nm) has the advantage of high precision for frequency standards [12, 13] and is a promising candidate for metrology. Measuring the hyperfine splitting of  $6P_{1/2}$  adds important input to theoretical calculations [7]. The hyperfine splitting measurement of  $6P$  states has been carried out using saturated absorption [14] for both  $6P_{1/2}$  and  $6P_{3/2}$  states, or fluorescence spectroscopy [15] for  $6P_{3/2}$  state on  $5S_{1/2} \rightarrow 6P_{3/2(1/2)}$  transition and using RF transition with electrical discharge [16].

The direct detection of absorption of 421 nm on  $5S_{1/2} \rightarrow 6P_{1/2}$  transition requires heating of Rb vapor cell upto  $80-100^\circ\text{C}$  [14, 17] and using a photodiode with

blue enhanced sensitivity. The spectroscopy at 421 nm can also be done using double-resonance spectroscopy [18–22] which does not require heating of Rb vapor cell. The double resonance method can be of electromagnetically induced transparency (EIT) type in a V-system [23–27] a technique which is known as coherent control spectroscopy (CCS). We have also added optical pumping technique for the same double resonance spectroscopy. The precise measurement of the hyperfine interval of  $6P_{1/2}$  state in  $^{87}\text{Rb}$  is carried out using the two double resonance spectroscopy methods. Although the method based upon electrical discharge in reference [16] provides great precision, it is important to measure hyperfine splitting with different methods to avoid systematic shifts in the experiment due to ion-atom and atom-atom collisions. Similarly heating the Rb cell also increases atom-atom collision and can cause collisional/pressure shift [28] which can contribute to systematic shift in the hyperfine measurement.

## II. MEASUREMENT SCHEMES

### A. Coherent Control Scheme

The energy level diagram for coherent control scheme is given in Fig. 1a and the experimental setup is as shown in Fig. 2. The 780 nm probe laser is locked to resonance on  $5S_{1/2}(F=2) \rightarrow 5P_{3/2}(F'=3)$  cycling transition and its absorption is monitored as the co-propagating 421 nm control laser beam scans  $5S_{1/2}(F=2) \rightarrow 6P_{1/2}$  transitions. As soon as the 421 nm scanning control laser comes to resonance (i.e. when both laser beams are addressing zero velocity group atoms), absorption of the 780 nm probe laser is reduced giving rise to a Doppler-free dip. There are two reasons for reduction of the 780 nm probe laser absorption. One is due to coherent effect i.e. V system EIT [24, 27] and another is optical pumping to other ground hyperfine level,  $5S_{1/2}(F=1)$  [29–31] via  $5S_{1/2}(F=2) \rightarrow 6P_{1/2}$  excitation and  $6P_{1/2} \rightarrow 5S_{1/2}(F=1)$  decay channels. The

\*Electronic address: kanhaiyapandey@iitg.ac.in

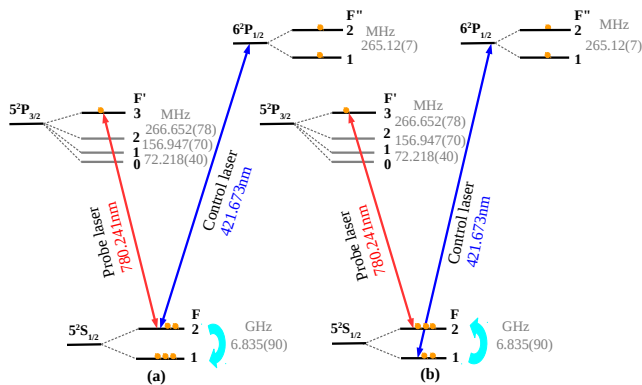


Figure 1: (Color online). Schematic of a multilevel atomic system interacting with two laser beams in (a) V-type scheme and (b) optical pumping scheme in  $^{87}\text{Rb}$ .

transparency spectrum is shown in Fig. 3a.

Besides the two hyperfine peaks due to zero velocity group atoms, there are other extra peaks outside the main spectrum. The extra peaks are caused by atoms moving with velocities 208 m/s and 330 m/s respectively. Atoms moving with velocity 208 m/s will see the 780 nm probe laser to be on resonance with  $5S_{1/2}(F=2) \rightarrow 5P_{3/2}(F'=2)$  transition. The corresponding two extra peaks are separated by hyperfine interval of  $6P_{1/2}$  and located at 494 MHz from the main peaks respectively. Similarly, atoms moving with velocity 330 m/s will be resonant for  $5S_{1/2}(F=2) \rightarrow 5P_{3/2}(F'=1)$  transition and another two fold of extra peaks are located at 783 MHz from the main peaks. The theoretical plot in Fig. 3 is generated using density matrix calculation for seven-level system in Doppler-broadened Rb atomic vapors at room temperature (300 K). Due to non-linearity in the scan of the laser, there is a mismatch between experiment and theory in the position of the extra peaks. The linewidth of the experimental spectrum ranges between 29 and 31 MHz and the theoretical simulation curve has a linewidth of 26 MHz. However, this linewidth is larger than the natural linewidth ( $6.065 + 1.27$  MHz). This is caused by Doppler mismatch between the 780 nm and 421 nm lasers [32].

### B. Optical Pumping Scheme

Fig. 1b is the energy level diagram for optical pumping scheme and the experimental setup is also given in Fig. 2. The 780 nm probe laser is locked to resonance on  $5S_{1/2}(F=2) \rightarrow 5P_{3/2}(F'=3)$  cycling transition and its absorption is monitored as the co-propagating 421 nm control laser beam scans around the  $6P_{1/2}$  hyperfine levels on  $5S_{1/2}(F=1) \rightarrow 6P_{1/2}$  transition instead of  $5S_{1/2}(F=2) \rightarrow 6P_{1/2}$  transition. The 421 nm scanning control laser beam, partially transfers population from the lower ground hyperfine level ( $5S_{1/2}(F=1)$ )

to the upper ground hyperfine level ( $5S_{1/2}(F=2)$ ) via  $5S_{1/2}(F=1) \rightarrow 6P_{1/2}$  excitation and  $6P_{1/2} \rightarrow 5S_{1/2}(F=2)$  decay channels. Thus, optical pumping of zero velocity group atoms to the upper ground hyperfine level [29–31] and coherence dephasing rate of the ground hyperfine levels [33–35] increase absorption of the probe giving rise to Doppler-free peaks. The absorption spectrum is shown in Fig. 3b. Since all velocity group atoms are optically pumped from  $5S_{1/2}(F=1)$  to  $5S_{1/2}(F=2)$  ground hyperfine level, extra peaks are formed outside the main spectrum as explained in the previous section. The linewidth of the experimental spectrum ranges between 29 and 34 MHz and linewidth for theoretical simulation curve is 23 and 34 MHz.

## III. EXPERIMENTAL DETAILS

### A. Setup and Results

The 780 nm beam is generated from (thorlab laser diode L785H1) a home-assembled extended cavity diode laser (ECDL) with typical linewidth of 500 kHz. The error signal for locking the 780 nm laser is generated by frequency modulation using the current of ECDL at 50 kHz. The error is fed to the piezo using a home-made analog PID controller for locking to the particular transition. The 421 nm beam is generated from commercial available ECDL from TOPTICA with model no. DL PRO HP with output power of 70 mW and linewidth of <200 kHz. In the experimental setup given in Fig. 2, the 421 nm laser beam addressing  $6P_{1/2}$  hyperfine level is divided into two laser beams. The first laser beam is passed directly through the Rb vapor cell and co-propagates with one of the 780 nm probe laser. The second 421 nm laser beam is passed through the acousto-optic modulator (AOM) twice and its frequency is shifted to be approximately the hyperfine interval value. The double-pass AOM configuration has the advantage of preserving the direction of propagation of the laser beam as the frequency of AOM is changed [36]. The AOM frequency in our double-pass setup is shifted between 130 – 136 MHz. The double passed AOM beam, again passes through the same Rb vapor cell where it co-propagate with the second 780 nm probe laser. The two sets of co-propagating 421 nm and 780 nm laser are around 12 mm apart in the same cell. The single-mode operation of the 421 nm laser is monitored using Confocal Fabry Perot Interferometer with free spectral range of 150 MHz. The beam diameter of the 780 nm probe laser is  $2 \times 3$  mm with measured power of  $42 \mu\text{W}$  (or intensity,  $I = 1.78 \text{ mW/cm}^2$  and corresponding Rabi frequency of  $2\pi \times 4.27$  MHz). The beam diameter of the 421 nm control laser is  $3 \times 4$  mm with measured power of 0.945 mW and calculated intensity,  $I = 20.05 \text{ mW/cm}^2$ . The intensity corresponds to Rabi frequency of  $2\pi \times 1.17$  MHz using the dipole moment in reference [11]

The spectrum of  $5S_{1/2}(F=2) \rightarrow 6P_{1/2}$  or  $5S_{1/2}(F=$

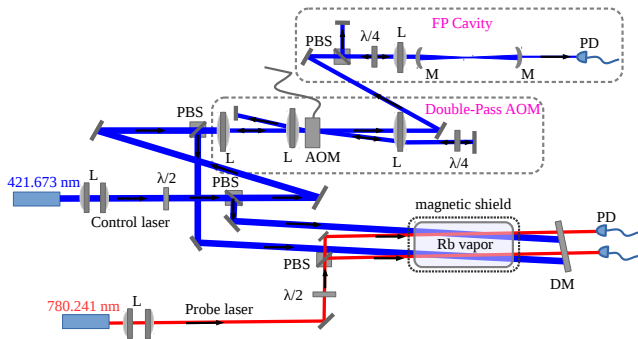


Figure 2: (Color online). Experimental setup for measuring hyperfine structure using coherent control and optical pumping schemes. L: Plano-convex lens;  $\lambda/2$ : half-wave plate;  $\lambda/4$ : quarter-wave plate; M: confocal mirror; DM: Dichroic mirror; PBS: polarization beam splitter; PD: photo-diode; AOM: acousto-optic modulator; FP: Fabry Perot cavity.

1)  $\rightarrow 6P_{1/2}$  weak transition driven by 421 nm laser shown in Fig. 3a and 3b respectively, is recorded using a picoscope through the changes in the absorption spectrum of 780 nm probe laser driving  $5S_{1/2}(F=2) \rightarrow 5P_{3/2}(F'=3)$  strong transition. The red and black traces of experimental spectrum in Fig. 4 corresponds to unshifted and shifted AOM beams respectively. One of the traces is deliberately inverted to see the matching of the two hyperfine peaks for the shifted and unshifted spectrum. The matching of the peaks is a measure of shifting the frequency of the laser beam by exactly the hyperfine interval. The frequency difference ( $\Delta_{\text{diff}}$ ) between the two peaks being matched is obtained by fitting the peaks with a Lorentzian line profile (see Fig. 4) and finding the difference in the peaks location. Fig. 5 shows a plot of frequency shift ( $2 \times$  AOM frequency) vs the frequency difference between the two peaks ( $\Delta_{\text{diff}}$ ). The hyperfine interval is obtained using a linear fit on the plot of frequency shift vs  $\Delta_{\text{diff}}$ . The frequency shift corresponding to zero frequency difference ( $\Delta_{\text{diff}} = 0$ ) in the linear fit is the hyperfine interval ( $\mathcal{V}_{\text{hfs}}$ ). This method removes the error due to scan non-linearity and hence improves the precision of measurement. From the linear fit the value of  $\mathcal{V}_{\text{hfs}} = 265.134 \pm 0.047$  MHz in the case of the coherent control scheme and  $\mathcal{V}_{\text{hfs}} = 265.196 \pm 0.034$  MHz for the optical pumping scheme.

## B. Errors

### 1. Systematic Errors

The main source of the systematic errors is the light shift and stray magnetic field through Zeeman shift. The systematic error arising due to stray magnetic field is minimized using a  $\mu$ -metal magnetic shield around the Rb cell. The residual fields is below 1 mG which corre-

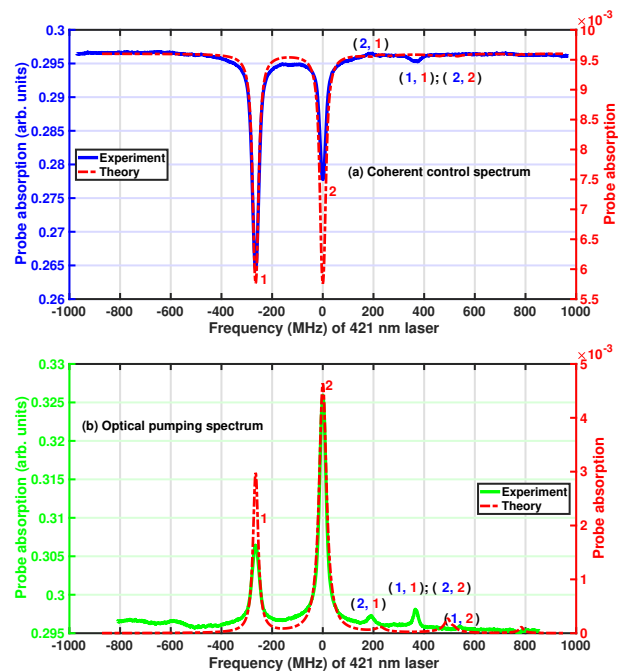


Figure 3: (Color online). Theoretical and experimental spectrum of  $6P_{1/2}$ . Extra peaks are caused by atoms moving with velocity 208 m/s and 330 m/s which brings 780 nm and 421 nm lasers to resonance on  $5S_{1/2}(F=2) \leftrightarrow 5P_{3/2}(F'=1,2)$  (blue color) and  $5S_{1/2}(F=1(2)) \leftrightarrow 6P_{1/2}(F''=1,2)$  transition (red color).

sponds to errors less than 1 kHz. The light shift error is due to presence of the hyperfine levels and the lasers driving simultaneously many levels off resonance causing the light shift of the levels driven resonantly. The locked probe laser  $5S_{1/2}(F=2) \rightarrow 5P_{3/2}(F'=3)$  cycling transition, also drives  $5S_{1/2}(F=2) \rightarrow 5P_{3/2}(F'=2(1))$  transitions off resonance causing the light shift to the ground state  $5S_{1/2}(F=2)$  upward and excited state  $5P_{3/2}(F=3)$  downwards. However, this shift does not cause any error for hyperfine interval because it will cause equal shift in the resonance for both the hyperfine levels of  $6P_{1/2}$ . The scanning control laser is the source of systematic error in the measurement of hyperfine interval. This is because, when it is resonant to  $5S_{1/2}(F=2) \rightarrow 6P_{1/2}(F''=1)$ , it also driving the  $5S_{1/2}(F=2) \rightarrow 6P_{1/2}(F''=2)$  off resonance (negative detuning equal to hyperfine interval,  $\mathcal{V}_{\text{hfs}}$ ) causing the ground state  $5S_{1/2}(F=2)$  to shift downwards by  $\Omega^2/4\mathcal{V}_{\text{hfs}}$ . This effect causes resonant frequency for  $5S_{1/2}(F=2) \rightarrow 6P_{1/2}(F''=1)$  to be shifted by  $+\Omega^2/4\mathcal{V}_{\text{hfs}}$ . Similarly, when the control laser is at resonance on  $5S_{1/2}(F=2) \rightarrow 6P_{1/2}(F''=2)$  transition, it is also driving the  $5S_{1/2}(F=2) \rightarrow 6P_{1/2}(F''=1)$  transition off resonance (positive detuning equal to hyperfine interval) causing the ground state  $5S_{1/2}(F=2)$  to shift upwards by  $\Omega^2/4\mathcal{V}_{\text{hfs}}$ . This causes resonant frequency for

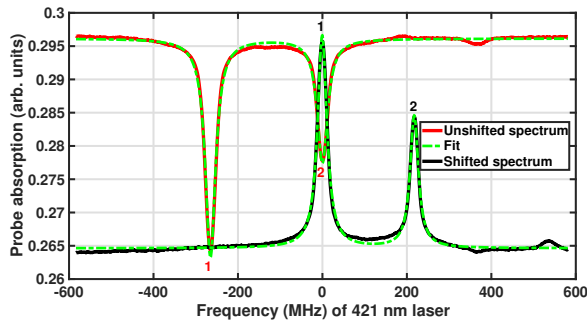


Figure 4: (Color online). Spectrum of shifted (black color) and unshifted (red color) beams fitted with a Lorentzian line profile (dashed green color) to obtain frequency difference ( $\Delta_{\text{diff}}$ ) between the matched peaks.

$5S_{1/2}(F = 2) \rightarrow 6P_{1/2}(F'' = 2)$  transition to be shifted by  $-\Omega^2/4\nu_{\text{hfs}}$ . The overall light shift error calculated using the laser intensities in the previous section is 13 kHz and 6 kHz for the coherent control scheme and the optical pumping scheme respectively.

## 2. Statistical Error

The above systematic error is much smaller than the statistical error in the experiment. The non-linear scan of the laser is the main cause the statistical error. This error is minimized by shifting AOM frequency within a small range of frequencies around the neighboring hyperfine level. To quantify the statistical error, two traces (shifted and unshifted spectrum) are recorded on two input channels of the picoscope with averaging of 20. Three such samples are taken for each AOM frequencies and the spread of the data ( $\Delta_{\text{diff}}$ ) is shown by the histogram in the inset of Fig. 5. The spread of the data gives the statistical error in the experiment and is extracted from the histogram using a Gaussian fit. The extracted statistical error is 0.326 MHz for the coherent control scheme and 0.337 MHz for the optical pumping scheme.

Table I: Hyperfine interval ( $\nu_{\text{hfs}}$ ) and magnetic dipole constant A for  $6P_{1/2}$  state in  $^{87}\text{Rb}$ . The number indicated in normal bracket is the statistical plus fitting error and in curly bracket is systematic error.

	$\nu_{\text{hfs}}$ (MHz)	A (MHz)	Reference
Coherent control	265.134(373){14}	132.567(200)	This work
Optical pumping	265.196(371){7}	132.598(200)	This work
	265.150(460)	132.83(500)	[14]
	265		[37]
		132.56(3)	[16, 38]

In summary, the statistical error is dominating over

systematic errors (light shift and stray magnetic field errors) and fitting error. The total error is 0.387 MHz and 0.378 MHz for the coherent control scheme and the

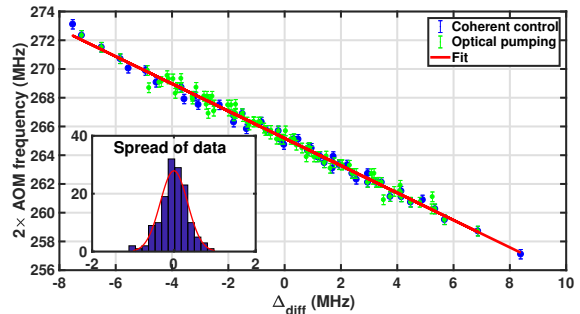


Figure 5: (Color online). A plot of frequency shift ( $2 \times$  AOM frequency) vs frequency difference ( $\Delta_{\text{diff}}$ ) for the two schemes. The inset shows the spread of data from the mean hyperfine interval.

optical pumping scheme respectively. Hence the hyperfine interval in the case of coherent control scheme is  $\nu_{\text{hfs}} = 265.134(373)\{14\}$  MHz and optical pumping scheme is  $\nu_{\text{hfs}} = 265.196(371)\{7\}$  MHz. The measured hyperfine interval is related to the magnetic dipole hyperfine constant,  $A = \nu_{\text{hfs}}(F \rightarrow F - 1)/F$ . The values of A are 132.567(200) MHz and 132.598(200) MHz for the two schemes respectively. A comparison of hyperfine interval ( $\nu_{\text{hfs}}$ ) and magnetic dipole constant A with the earlier works is given in Tab. I.

## IV. CONCLUSIONS

We have presented two experimental schemes for precision measurement of hyperfine interval of  $6P_{1/2}$  state of  $^{87}\text{Rb}$ , namely coherent control and optical pumping schemes using double resonance at 780 nm and 421 nm. Using an AOM, we have taken care of the scan non-linearity which is the dominant source of error in the experiment. The measured hyperfine interval is consistent with two other techniques namely saturated absorption and electrical discharge within the precision of our measurement.

## Acknowledgement

E.O.N. would like to acknowledge Indian Council for Cultural Relations (ICCR) for the PhD scholarship. K.P. would like to acknowledge the funding from SERB of grant No. ECR/2017/000781.

- [1] J. Ye, S. Swartz, P. Jungner, and J. L. Hall, *Opt. Lett.* **21**, 1280 (1996), URL <http://ol.osa.org/abstract.cfm?URI=ol-21-16-1280>.
- [2] A. Marian, M. C. Stowe, D. Felinto, and J. Ye, *Phys. Rev. Lett.* **95**, 023001 (2005), URL <https://link.aps.org/doi/10.1103/PhysRevLett.95.023001>.
- [3] A. Banerjee and V. Natarajan, *Phys. Rev. A* **70**, 052505 (2004), URL <https://link.aps.org/doi/10.1103/PhysRevA.70.052505>.
- [4] D. Touahri, O. Acef, A. Clairon, J.-J. Zondy, R. Felder, L. Hilico, B. de Beauvoir, F. Biraben, and F. Nez, *Optics Communications* **133**, 471 (1997), ISSN 0030-4018, URL <http://www.sciencedirect.com/science/article/pii/S0030401896004713>.
- [5] P. Morzyński, P. Weisło, P. Ablewski, R. Gartman, W. Gawlik, P. Masłowski, B. Nagórny, F. Ozimek, C. Radzewicz, M. Witkowski, et al., *Opt. Lett.* **38**, 4581 (2013), URL <http://ol.osa.org/abstract.cfm?URI=ol-38-22-4581>.
- [6] H.-C. Chui, M.-S. Ko, Y.-W. Liu, J.-T. Shy, J.-L. Peng, and H. Ahn, *Opt. Lett.* **30**, 842 (2005), URL <http://ol.osa.org/abstract.cfm?URI=ol-30-8-842>.
- [7] M. S. Safronova and U. I. Safronova, *Phys. Rev. A* **83**, 052508 (2011), URL <https://link.aps.org/doi/10.1103/PhysRevA.83.052508>.
- [8] C.-B. Li, Y.-M. Yu, and B. K. Sahoo, *Phys. Rev. A* **97**, 022512 (2018), URL <https://link.aps.org/doi/10.1103/PhysRevA.97.022512>.
- [9] M. S. Safronova and U. I. Safronova, *Phys. Rev. A* **83**, 012503 (2011), URL <https://link.aps.org/doi/10.1103/PhysRevA.83.012503>.
- [10] M. S. Safronova, D. Budker, D. DeMille, D. F. J. Kimball, A. Derevianko, and C. W. Clark, *Rev. Mod. Phys.* **90**, 025008 (2018), URL <https://link.aps.org/doi/10.1103/RevModPhys.90.025008>.
- [11] M. S. Safronova, C. J. Williams, and C. W. Clark, *Phys. Rev. A* **69**, 022509 (2004), URL <https://link.aps.org/doi/10.1103/PhysRevA.69.022509>.
- [12] S.-N. Zhang, X.-G. Zhang, J.-H. Tu, Z.-J. Jiang, H.-S. Shang, C.-W. Zhu, W. Yang, J.-Z. Cui, and J.-B. Chen, *Chinese Physics Letters* **34**, 074211 (2017), URL <https://doi.org/10.1088/2F0256-307x%2F34%2F7%2F074211>.
- [13] S. Zhang, P. Chang, H. Shang, and J. Chen, in *2018 IEEE International Frequency Control Symposium (IFCS)* (IEEE, 2018), pp. 1–4.
- [14] C. Glaser, F. Karlewski, J. Grimmel, M. Kaiser, A. Gänther, H. Hattermann, and J. Fortágh, *Absolute frequency measurement of rubidium 5s-6p transitions* (2019), 1905.08824.
- [15] J. Navarro-Navarrete, A. Díaz-Calderón, L. Hoyos-Campo, F. Ponciano-Ojeda, J. Flores-Mijangos, F. Ramírez-Martínez, and J. Jiménez-Mier, arXiv preprint arXiv:1906.07114 (2019).
- [16] D. Feiertag and G. Zu Putlitz, *Zeitschrift für Physik A Hadrons and nuclei* **261**, 1 (1973).
- [17] S. Pustelny, L. Busaite, M. Auzinsh, A. Akulshin, N. Leefer, and D. Budker, *Phys. Rev. A* **92**, 053410 (2015), URL <https://link.aps.org/doi/10.1103/PhysRevA.92.053410>.
- [18] J. R. Boon, E. Zekou, D. J. Fulton, and M. H. Dunn, *Phys. Rev. A* **57**, 1323 (1998), URL <https://link.aps.org/doi/10.1103/PhysRevA.57.1323>.
- [19] A. Nishiyama, S. Yoshida, Y. Nakajima, H. Sasada, K. Nakagawa, A. Onae, and K. Minoshima, *Opt. Express* **24**, 25894 (2016), URL <http://www.opticsexpress.org/abstract.cfm?URI=oe-24-22-25894>.
- [20] F. Ponciano-Ojeda, C. Mojica-Casique, S. Hernández-Gómez, O. López-Hernández, L. M. Hoyos-Campo, J. Flores-Mijangos, F. Ramírez-Martínez, D. Sahagún, R. Jáuregui, and J. Jiménez-Mier, *Journal of Physics B: Atomic, Molecular and Optical Physics* **52**, 135001 (2019), URL <https://doi.org/10.1088/2F1361-6455%2F52%2F135001>.
- [21] M. Suzuki and S. Yamaguchi, *IEEE Journal of Quantum Electronics* **24**, 2392 (1988).
- [22] F. Bylicki, G. Persch, E. Mehdizadeh, and W. Demtröder, *Chemical Physics* **135**, 255 (1989), ISSN 0301-0104, URL <http://www.sciencedirect.com/science/article/pii/0301010489870259>.
- [23] A. Banerjee and V. Natarajan, *Opt. Lett.* **28**, 1912 (2003), URL <http://ol.osa.org/abstract.cfm?URI=ol-28-20-1912>.
- [24] D. Das and V. Natarajan, *EPL (Europhysics Letters)* **72**, 740 (2005), URL <http://stacks.iop.org/0295-5075/72/i=5/a=740>.
- [25] D. Das and V. Natarajan, *Journal of Physics B: Atomic, Molecular and Optical Physics* **41**, 035001 (2008), URL <http://stacks.iop.org/0953-4075/41/i=3/a=035001>.
- [26] D. Das, K. Pandey, A. Wasan, and V. Natarajan, *Journal of Physics B: Atomic, Molecular and Optical Physics* **39**, 3111 (2006), URL <http://stacks.iop.org/0953-4075/39/i=14/a=017>.
- [27] S. Menon and G. S. Agarwal, *Phys. Rev. A* **61**, 013807 (1999), URL <https://link.aps.org/doi/10.1103/PhysRevA.61.013807>.
- [28] W. Xia, S.-Y. Dai, Y. Zhang, K.-Q. Li, Q. Yu, and X.-Z. Chen, *Chinese Physics Letters* **33**, 053201 (2016), URL <https://doi.org/10.1088/2F0256-307x%2F33%2F5%2F053201>.
- [29] M. S. Feld, M. M. Burns, T. U. Kühn, P. G. Pappas, and D. E. Murnick, *Opt. Lett.* **5**, 79 (1980), URL <http://ol.osa.org/abstract.cfm?URI=ol-5-2-79>.
- [30] D. A. Smith and I. G. Hughes, *American Journal of Physics* **72**, 631 (2004), <https://doi.org/10.1119/1.1652039>, URL <https://doi.org/10.1119/1.1652039>.
- [31] H. R. Noh, *European Journal of Physics* **30**, 1181 (2009), URL <http://stacks.iop.org/0143-0807/30/i=5/a=025>.
- [32] A. Urvoy, C. Carr, R. Ritter, C. S. Adams, K. J. Weatherill, and R. Löw, *Journal of Physics B: Atomic, Molecular and Optical Physics* **46**, 245001 (2013), URL <https://doi.org/10.1088/2F0953-4075%2F46%2F24%2F245001>.
- [33] D. J. Fulton, S. Shepherd, R. R. Moseley, B. D. Sinclair, and M. H. Dunn, *Phys. Rev. A* **52**, 2302 (1995), URL <https://link.aps.org/doi/10.1103/PhysRevA.52.2302>.
- [34] M. Manjappa, S. S. Undurti, A. Karigowda, A. Narayanan, and B. C. Sanders, *Phys. Rev. A* **90**, 043859 (2014), URL <https://link.aps.org/doi/10.1103/PhysRevA.90.043859>.
- [35] V. B. Tiwari, S. Singh, H. S. Rawat, M. P. Singh, and

- S. C. Mehendale, *Journal of Physics B: Atomic, Molecular and Optical Physics* **43**, 095503 (2010), URL <https://doi.org/10.1088/0953-4075/43/9/095503>.
- [36] E. A. Donley, T. P. Heavner, F. Levi, M. O. Tataw, and S. R. Jefferts, *Review of Scientific Instruments* **76**, 063112 (2005), <https://doi.org/10.1063/1.1930095>, URL <https://doi.org/10.1063/1.1930095>.
- [37] P. Grundevik, M. Gustavsson, A. Rosén, and S. Svanberg, *Zeitschrift für Physik A Atoms and Nuclei* **283**, 127 (1977), ISSN 0939-7922, URL <https://doi.org/10.1007/BF01418703>.
- [38] E. Arimondo, M. Inguscio, and P. Violino, *Rev. Mod. Phys.* **49**, 31 (1977), URL <https://link.aps.org/doi/10.1103/RevModPhys.49.31>.